



HAL
open science

Fission lifetime measured by the blocking technique as a function of excitation energy in the 24 A.MeV $^{238}\text{U} + ^{28}\text{Si}$ reaction

M. Morjean, M. Chevallier, C. Cohen, D. Dauvergne, J. Dural, J. Galin, F. Goldenbaum, D. Jacquet, R. Kirsch, E. Liénard, et al.

► To cite this version:

M. Morjean, M. Chevallier, C. Cohen, D. Dauvergne, J. Dural, et al.. Fission lifetime measured by the blocking technique as a function of excitation energy in the 24 A.MeV $^{238}\text{U} + ^{28}\text{Si}$ reaction. Sixth International Conference on Nucleus-Nucleus Collisions, Jun 1997, Gatlinburg, United States. pp.200c-208c. in2p3-00003441

HAL Id: in2p3-00003441

<https://hal.in2p3.fr/in2p3-00003441>

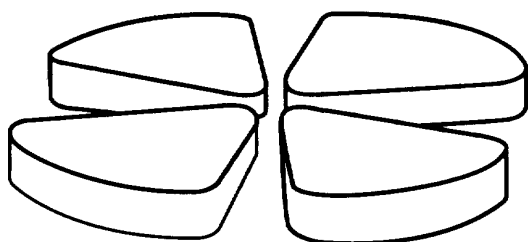
Submitted on 13 Jan 1999

HAL is a multi-disciplinary open access archive for the deposit and dissemination of scientific research documents, whether they are published or not. The documents may come from teaching and research institutions in France or abroad, or from public or private research centers.

L'archive ouverte pluridisciplinaire **HAL**, est destinée au dépôt et à la diffusion de documents scientifiques de niveau recherche, publiés ou non, émanant des établissements d'enseignement et de recherche français ou étrangers, des laboratoires publics ou privés.

BB

GANIL



FISSION LIFETIME MEASURED BY THE BLOCKING TECHNIQUE
AS A FUNCTION OF EXCITATION ENERGY IN THE 24 A.MeV
 $^{238}\text{U} + ^{28}\text{Si}$ REACTION

M. Morjean^a, M. Chevallier^b, C. Cohen^c, D. Dauvergne^b, J. Dural^e, J. Galin^a, F.
Goldenbaum^a, D. Jacquet^d, R. Kirsch^b, E. Lienard^a, B. Lott^a, A. Peghaire^a, Y. Perier^a,
J.C. Poizat^b, G. Prevot^c, J. Remillieux^b, D. Schmaus^c, M. Toulemonde^e

^aGANIL (DSM/CEA, IN2P3/CNRS),
BP 5027, 14076 Caen Cedex 5, France

^bInstitut de Physique Nucléaire de Lyon, IN2P3/CNRS, Univ. Cl. Bernard,
43 Bd. 11 Novembre 1918, F-69622 Villeurbanne Cedex, France

^cGPS,
2 place Jussieu, 75251 Paris Cedex 05, France

^dInstitut de Physique Nucléaire d'Orsay,
BP 1, F-91406 Orsay Cedex, France

^eCIRIL,
BP 5133, 14040 Caen Cedex, France



CERN LIBRARIES, GENEVA

swg727

GANIL P 97 21

FISSION LIFETIME MEASURED BY THE BLOCKING TECHNIQUE AS A FUNCTION OF EXCITATION ENERGY IN THE 24 A.MeV $^{238}\text{U} + ^{28}\text{Si}$ REACTION

M. Morjean^a, M. Chevallier^b, C. Cohen^c, D. Dauvergne^b, J. Dural^c, J. Galin^a, F. Goldenbaum^a, D. Jacquet^d, R. Kirsch^b, E. Lienard^a, B. Lott^a, A. Peghaire^a, Y. Perier^a, J.C. Poizat^b, G. Prevot^c, J. Remillieux^b, D. Schmaus^c, M. Toulemonde^c

^aGANIL (DSM/CEA, IN2P3/CNRS),
BP 5027, 14076 Caen Cedex 5, France

^bInstitut de Physique Nucléaire de Lyon, IN2P3/CNRS, Univ. Cl. Bernard,
43 Bd. 11 Novembre 1918, F-69622 Villeurbanne Cedex, France

^cGPS,
2 place Jussieu, 75251 Paris Cedex 05, France

^dInstitut de Physique Nucléaire d'Orsay,
BP 1, F-91406 Orsay Cedex, France

^eCIRIL,
BP 5133, 14040 Caen Cedex, France

The blocking technique has been used to infer fission lifetimes as a function of excitation energy for uranium-like nuclei formed in the U+Si reactions at 24 MeV/nucleon. The fission lifetimes are found larger than 10^{-19}s for excitation energies up to about 250 MeV.

1. INTRODUCTION

The dissipation of collective energy into thermal excitation energy during the fission process can be inferred [1] from the time required by a nucleus to reach its scission configuration, time usually referred to as fission lifetime τ_{fiss} . Theoretical predictions for the magnitude of the dissipation coefficients vary by at least two orders of magnitude depending on the assumptions on the processes responsible for the dissipation. Furthermore, even the dependence of dissipation on temperature is not well known. Models based on the linear response theory predict an increase of dissipation as the temperature increases [2] whereas the dissipation calculated in a microscopic way assuming two-body viscosity [3] varies just in the opposite way in the same range of temperature. In order to get a better determination of the dissipation processes and thus information on the nuclear matter viscosity, an accurate experimental determination of the fission lifetime as a function of the temperature of the fissioning nucleus is essential.

Two main different experimental approaches have been followed so far to infer fission lifetimes. The first one measures pre- and post-fission particle [1] or GDR- γ [4] multiplicities and calculates the lifetimes associated with these multiplicities using statistical models. Unfortunately, very different lifetimes are inferred from these experiments depending on the probe used (neutrons or charged particles or γ rays), or even depending on assumptions made in the analysis of the same data [5]. The discrepancies between the data from the various probes could arise from the limited time windows actually accessible using a specific probe [6] or from uncertainties on parameters used in the statistical models (evolution of the level density parameters with temperature, deformation...). The second experimental approach, the so-called blocking technique [7], seems to be the most straightforward one because it is based mainly on simple calculations of electric potentials in single crystals. This technique, that will be discussed in more details in the next section, determines the distance from an atomic string or plane of a single crystal at which the scission occurs, provided this distance is not significantly smaller than the thermal vibration amplitudes of the crystal. Up to now, the experiments using this technique [8–12] could only discriminate between rather long lifetimes ($\tau_{fiss} \geq 10^{-17}$ s) due to the low velocity of the fissioning nuclei that prevented them from getting out of the range of thermal vibrations. The availability at GANIL of high quality ^{238}U beams accelerated at 24 MeV/nucleon makes it possible to study fission events induced in reverse kinematics. Therefore, it is the projectile-like nucleus (PLN), moving with a high velocity, that will undergo fission and much shorter lifetimes than in the previous experiments become then accessible. Furthermore, the fission fragments have also rather high velocities that permit their atomic number identification. In the present paper, the fission lifetimes have been investigated as a function of the excitation energy (inferred from the neutron multiplicity measured on 4π) for the $^{238}\text{U}+^{28}\text{Si}$ system at 24 MeV/nucleon.

2. EXPERIMENTAL PROCEDURE

2.1. Principle of the blocking technique

The discovery of blocking phenomena [13] in single crystals dates back 1965 and, immediately after, their application to nuclear lifetimes measurements was suggested [14]. The principle of fission lifetime measurement is presented in Fig. 1 where the crystal lattice is schematically represented by black dots. A beam is impinging on a single crystal used as a target and, when a nuclear reaction occurs between projectile and target nuclei, the nucleus that will undergo fission is imparted a recoil velocity. Depending on the time needed by this nucleus to reach its scission shape, a more or less large distance will be covered within the crystal before the two fission fragments get separated. If the lifetime is very short, a fission fragment initially emitted in the direction of an axis or plane of the crystal will be deflected away, as shown for trajectory labelled 1 in the figure, due to the high repulsive atomic field of the atomic string or plane. Therefore, the yield in the direction of axes or planes will be lower than in other directions. If the lifetime is longer, the fissioning nucleus will move far away from the atomic string or plane, in a region where the mean electric field is weaker. It will then suffer a smaller deflection, as shown for the trajectory labelled 2 in the picture. The blocking effect magnitude in the direction of axes or planes is hence a quite straightforward measurement of fission lifetime

based essentially on electrostatic calculations. Nevertheless, the main limitation of this technique arises from the thermal vibrations of the lattice that induce a smearing of the potential preventing discrimination between distances significantly smaller than about 0.075\AA (for silicon at 300K), leading to a lower limit for the times actually accessible.

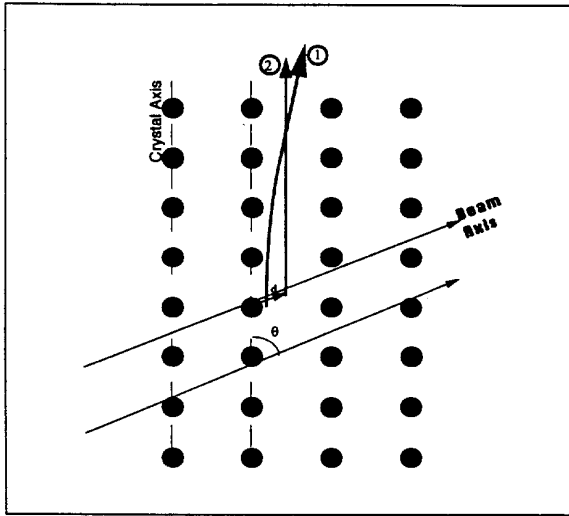


Figure 1. Principle of lifetime measurement by the blocking technique.

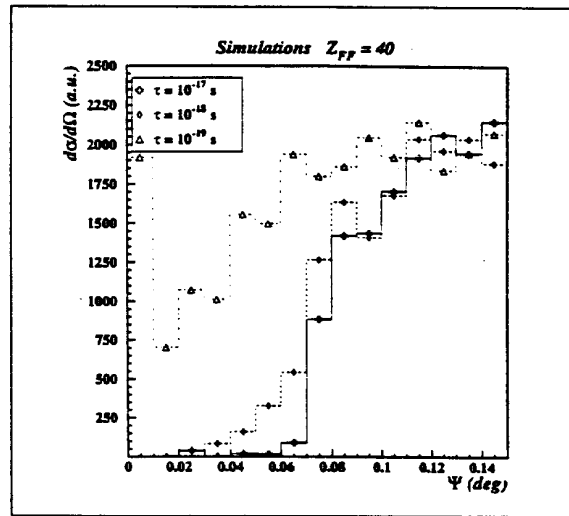


Figure 2. Results of simulations for fission fragment angular distributions with respect to the $\langle 110 \rangle$ axis of a single silicon crystal.

The main originality of the present work is to take advantage of the high velocity ^{238}U projectiles available at GANIL at 24 MeV/nucleon to induce reactions in which the PLN undergoes fission. The limit of the blocking technique is then pushed ahead as compared to previous experiments in which fission fragments of the slowly moving target-like fragments were detected. Simulations of the blocking effects have been performed for the $^{238}\text{U} + ^{28}\text{Si}$ system at 24 MeV/nucleon. In these simulations, an isotropic emission in the PLN frame is assumed for fission fragments with a velocity taken according to the systematics of V. Viola [15] and the PLN velocity and angular distributions are taken from reference [16]. Fig. 2 presents the angular distributions around 7 deg with respect to the beam axis for fission fragments emerging at an angle Ψ with respect to the $\langle 110 \rangle$ axis. The angular distributions have been calculated using the potential from L'Hoir et al. [17] and assuming exponential distributions for the fission lifetimes with various average times. A good discrimination is observed for average lifetimes longer than 10^{-19}s provided the experimental angular resolution is better than about 10^{-2}deg . Despite the focussing effect of the fission fragments in forward direction, this limit for time discrimination is one order of magnitude shorter than the one that would have been reached using non-reverse kinematics.

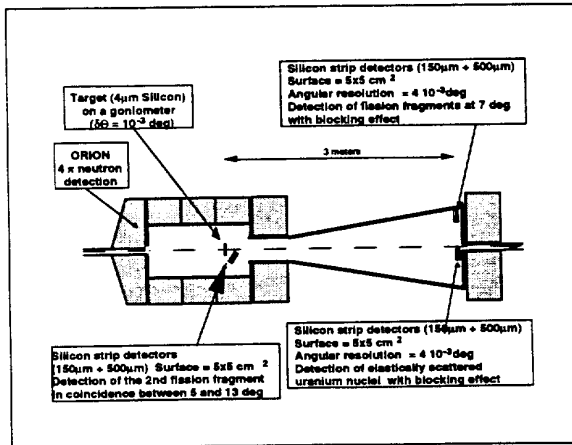


Figure 3. Experimental set-up.

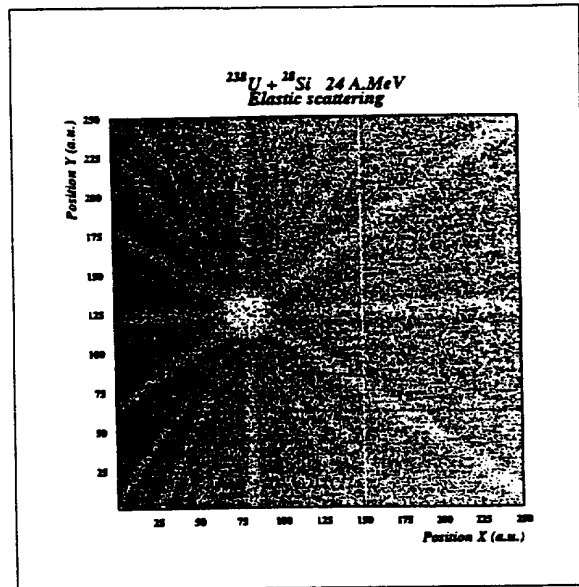


Figure 4. Two-dimensional blocking pattern around the $\langle 110 \rangle$ axis obtained around 1 deg for elastically scattered uranium nuclei.

2.2. Experimental set-up

A ^{28}Si single crystal with an effective thickness $5.8 \mu\text{m}$ was mounted on a goniometer inside a reaction chamber and bombarded with a $24 \text{ MeV/nucleon } ^{238}\text{U}$ beam. The experimental set-up is presented in Fig. 3. At 3 meters downstream from the target were located 2 telescopes, constituted of 2 large area ($5 \times 5 \text{ cm}^2$) silicon strip detectors each. The first detector of each telescope was $150 \mu\text{m}$ thick, made of 250 vertical strips whereas the second one was $500 \mu\text{m}$ thick with 250 horizontal strips. The spacing between two adjacent strips was $200 \mu\text{m}$ and the detected fragment position was determined by a charge division technique leading to a precision equivalent to a single strip width ($\pm 2 \cdot 10^{-3} \text{ deg}$). One of the two telescopes was located at 7 deg with respect to the beam axis in order to measure, for fission fragments emitted in this direction, the dip in the angular distribution due to the blocking effect when the $\langle 110 \rangle$ axis of the crystal was set with the goniometer at this angle. The second telescope was located at 1 deg with respect to the beam axis and detected mainly elastically scattered uranium nuclei. During the whole experiment, short periods of beam time were devoted to measurements in which the $\langle 110 \rangle$ crystal axis was set in the direction of this telescope in order to determine the dip associated with the very fast Rutherford scattering process. Any variation during the experiment of the shape of this dip would have been an indication of beam radiation damages, but no significant evolution has been observed with a beam intensity of about 10^7 ions per second during 8 days. A third telescope, located at 20 cm from the target, covered angles between -5 and -13 deg in order to detect with a large angular acceptance

the coincident fission fragment. The atomic number identification has been achieved by the ΔE - E technique up to $Z=50$.

The reaction chamber was surrounded by ORION, a 4π neutron detector constituted of 5 m^3 of liquid scintillator loaded with gadolinium. The efficiency of such detectors depends on the neutron kinetic energy and direction. For an isotropic emission from a PLN with a velocity close to the beam velocity, Monte-Carlo simulations [18] of the neutron capture indicate an efficiency $\epsilon \approx 50\%$.

2.3. Excitation energy determination

The excitation energy was inferred from the neutron multiplicity measured event-by-event by ORION. This detector is divided in 6 independent sectors along the beam axis, providing us with a rough angular distribution of the detected neutrons. An estimation of the overall contribution from neutrons emitted by the target-like fragment has then been made. This contribution is found very weak whatever the violence of the collision is (less than 1 neutron for the most dissipative collisions). The correlation between excitation energy and neutron multiplicity has been calculated using the statistical code PACE [19] for excited nuclei that do not undergo fission. In order to take into account the neutrons gained during the fission process itself, 2 extra neutrons have been added to the neutron multiplicity associated with a nucleus that do not undergo fission [20]. The uncertainties on the excitation energies that will be presented in the following include a ± 1 neutron error on this latter correction.

3. RESULTS

A typical picture of the blocking effects as measured for elastically scattered uranium nuclei detected by the telescope located at 1 deg is presented in Fig. 4. The cross section exhibits the overall angular evolution expected for Rutherford scattering except in the region in which the blocking effects due to the $\langle 110 \rangle$ axis as well as to various planes of the crystal can be clearly identified. A extinction yield of about 98% is found in the axis direction, as expected for an almost perfect crystal.

The angular distributions $d\sigma/d\Omega$ obtained with the telescope located at 7 deg, when two fission fragments are detected in coincidence, have been integrated over the azimuthal angles as a function of the Ψ angle with respect to the $\langle 110 \rangle$ axis and are presented in Fig. 5 for bins in neutron multiplicity. The dips associated with low neutron multiplicities are much less pronounced than the ones associated with high excitation energies, a strong indication of the shorter lifetimes associated with fission at high excitation energy. When moving away from the crystal axis towards large Ψ values, an almost constant cross-section $d\sigma/d\Omega$ is reached and, in the following, the blocking ratio \mathcal{R} between the yield inside the dip (integrated up to half the constant value at large angles) and the yield integrated over the whole detection range will be considered as representative of the blocking effect magnitude.

The evolution of \mathcal{R} with the excitation energy E^* is presented in Fig. 6. The excitation energy has been inferred following the procedure given in the previous chapter. The PLN atomic number before fission is $Z_{PLN} = 92 \pm 2$ [16] for detected neutron multiplicity $M_n < 10$, corresponding to $E^* < 250 \text{ MeV}$. For higher excitation energies, Z_{PLN} slowly increases up to the compound nucleus atomic number [16], reached when the total available

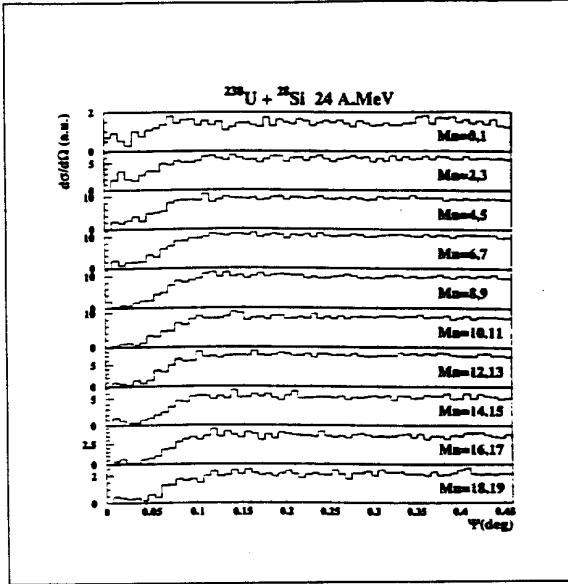


Figure 5. Angular distribution with respect to the $\langle 110 \rangle$ axis for bins in neutron multiplicity (no correction has been applied for neutron detection efficiency). The distributions are averaged over the azimuthal angles

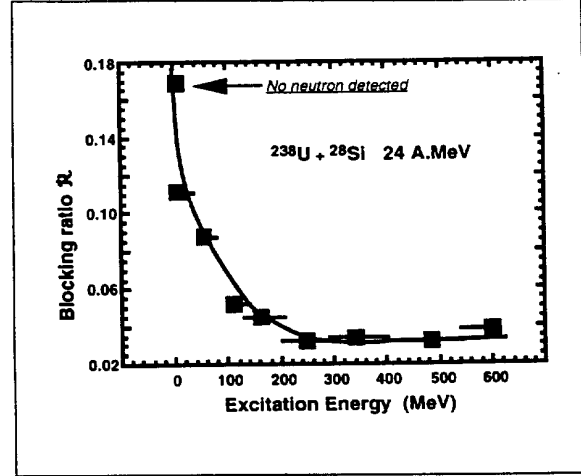


Figure 6. Blocking effect magnitude as a function of the excitation energy of the fissioning projectile-like fragment.

energy (~ 600 MeV) has been converted into excitation energy. The most striking feature of Fig. 6 is the strong evolution observed for excitation energies lower than 250 MeV, followed by an almost constant \mathcal{R} for the highest excitation energies. This evolution can be compared with the one obtained from simulations (Fig. 7) assuming for fission lifetimes an exponential distribution with an average time τ . In order to check whether the blocking technique is only sensitive to long lifetime components, as often believed, Fig. 7 presents also the results of simulations performed assuming a very narrow gaussian fission lifetime distribution, with average lifetimes τ and widths taken arbitrarily as $\sigma = \tau/10$. Despite the very different distribution shapes, the ratio \mathcal{R} is mainly sensitive to the average lifetime τ and not only to the long lifetime tail of the exponential distribution. Whatever the time distribution is, a fast evolution is observed in Fig. 7 when τ decreases down to 10^{-19} s, followed by a constant \mathcal{R} value for smaller times. This constant value results from the potential averaging due to the thermal vibrations of the crystal (see previous chapter). Considering these simulations, the strong evolution observed for $E^* < 250$ MeV can only be reproduced with average fission lifetimes longer than 10^{-19} s. In fact, the lifetimes associated with $E^* < 250$ MeV could even be longer than 10^{-19} s if one considers the effect of post-scission neutrons on the angular distributions. Monte-Carlo simulations show that the actual effect of post-scission neutrons on \mathcal{R} is quite negligible as long as the evaporation after scission is faster than 10^{-17} s: it leads to an isotropic modification of the angular distribution for fission fragments that did not have time enough to move

away from their scission point within the crystal transverse lattice. However, this effect becomes more and more significant for longer evaporation times as shown in Fig. 8 where a systematic emission of one neutron at 10^{-16} s after scission has been included in the simulations. Although a neutron emission at this very late stage of the process should have a low probability, Fig. 8 shows that the limit for discrimination is slightly increased toward longer times. Such long fission lifetimes are one or two orders of magnitude larger than the ones inferred from pre- and post-fission neutron multiplicities [21] and are even longer than the ones inferred from GDR- γ multiplicities [22,23] for similar nuclei and excitation energies. They should imply very high viscosity for hot nuclear matter.

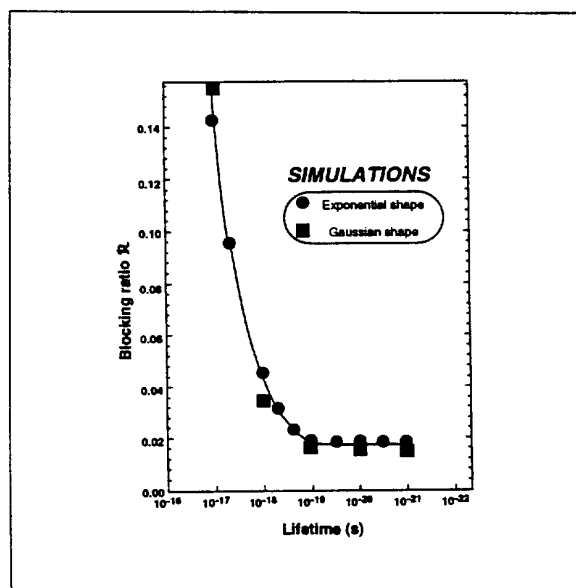


Figure 7. Blocking effect magnitude from simulations assuming either an exponential distribution for the fission lifetimes or a gaussian distribution.

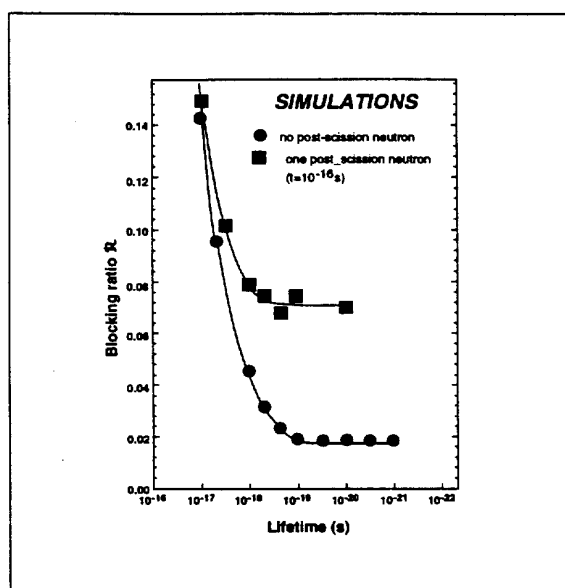


Figure 8. Blocking effect magnitude from simulations including the effect of one neutron emitted for each fission event 10^{-16} s after scission.

At very low E^* , two different values of \mathcal{R} are presented for the same initial PLN excitation in Fig. 6. The highest value, corresponding to a longer lifetime, is associated with events in which no neutron has been detected, whereas the lowest value is associated with one neutron detected (two neutrons after correction for detection efficiency). On the average, two extra neutrons are emitted during the fission process of uranium-like nuclei [20], but this neutron number depends on the actual shape of the fissioning nucleus at the scission point. For a very small part of the cross-section, a very compact shape is observed for which the fission fragments at the scission point are produced with an almost spherical shape, leading to no post-scission neutron. These events are usually referred to as cold fission events. In our experiment, a significant proportion of the fission events

detected without any neutron arises from the finite neutron detection efficiency, but the strong increase of \mathcal{R} associated with no neutron detected can be an indication of a longer lifetime associated with the cold fission process. Compact shapes at the scission point could arise from shape fluctuations that need rather long times to develop.

4. CONCLUSIONS

The blocking technique has been used to infer fission lifetimes of uranium-like nuclei. Using a 24 MeV per nucleon ^{238}U beam and taking advantage of the large velocity of the high-fissility projectile-like fragments, shorter lifetimes could be accessed by this straightforward technique as compared to previous experiments. The average fission lifetime is found to decrease when the excitation energy increases up to 250 MeV. For higher excitation energies, the blocking patterns do not exhibit any evolution, most likely due to the discrimination limit of the experimental technique.

At low projectile-like fragment excitation energy, the time scale associated with events without any detected neutron is found longer than the one associated with fission processes in which post-scission neutrons are emitted. This effect could be due to the distribution of the fission fragment deformations at the scission point, leading for cold-fission events to almost spherical shapes. For excitation energies up to 250 MeV (or temperatures up to 3 MeV), the average lifetimes are found larger than 10^{-19}s , a much longer time than the ones inferred in previous experiment either from neutron, charged particle or GDR- γ multiplicities. Whatever the considered model for fission, these very long lifetimes imply very large dissipation coefficients and a very high viscosity for hot nuclear matter.

We would like to acknowledge the help of R. Beunard, Y. Georget, J. Moulin, J.L. Vignet and A. Vigot before and during the experiment.

REFERENCES

1. D. Hilscher and H. Rossner, *Ann. Phys. Fr.* 17 (1992) 471
2. S. Yamiji et al., *Nucl. Phys.* A612 (1997) 1
3. D. Boilley et al., *Nucl. Phys.* A556 (1993) 67
4. P. Paul and M. Thoennessen, *Ann. Rev. Part. Nuc. Sci.* 44 (1994) 65
5. K. Siwek-Wilczynska et al., *Phys. Rev.* C51 (1995) 2054
6. P. Fröhbrich et I.I. Gontchar, HMI preprint TV96-Frob2 (1996)
7. W.M. Gibson, *Ann. Rev. Nucl. Sci.* 25 (1975) 465
8. J.U. Andersen et al., *Nucl. Phys.* A241 (1975) 317
9. S.A. Karamyan et al., *Sov. J. Part. Nucl.* 4 (1973) 196
10. J.U. Andersen et al., *Phys. Rev. Lett.* 36 (1976) 1539
11. J.S. Forster et al., *Nucl. Phys.* A464 (1987) 497
12. V.N. Bugrov et al., *Sov. J. Nucl. Phys.* 44 (1986) 903
13. B. Domeij and K. Bjorkqvist, *Phys. Lett.* 14 (1965) 129
14. D.S. Gemmell and R.E. Holland, *Phys. Rev. Lett.* 14 (1965) 945
15. V.E. Viola, *Nucl. Data* 1 (1966) 391
16. E. Piasecki et al., *Phys. Lett.* B351 (1995) 412

17. A. L'Hoir et al., Nucl. Inst. and Meth. Phys. Res. B48 (1990) 145
18. J. Poitou and C. Signarbieux, Nucl. Inst. Meth. 114 (1974) 113
19. A. Gavron, Phys. Rev. C21 (1980) 230
20. R. Vandenbosch and J.R. Huizenga, Nuclear Fission (Academic Press, New York and London, 1973)
21. D.J. Hinde et al., Phys. Rev. C45 (1992) 1229
22. R. Butsch et al., Phys. Rev. C44 (1991) 1515
23. I. Dioszegi et al., Phys. Rev. C46 (1992) 627

.

.

.

.